

An Automated Optimal Design of a Fan Blade Using an Integrated CFD/MDO Computer Environment

Uyigüe Idahosa¹ and Vladimir V. Golubev²
Embry-Riddle Aeronautical University, Daytona Beach, FL 32127

Vladimir O. Balabanov³
Vanderplaats Research and Development, Inc., Colorado Springs, CO 80906

The work discusses construction and application of an automated, distributed, industry-like multi-disciplinary design optimization (MDO) environment employed to explore new conceptual designs of propulsion system turbomachinery components optimized for high-efficiency performance. The integrated CFD/MDO system is developed on the basis of commercially available optimization modules, and involves a user-friendly interface that provides an easy link to user-supplied response analysis modules. Various issues in the automated optimization procedure are addressed with focus on turbomachinery design, including the proper geometry parameterization, algorithm selection, and transparent interconnections between different elements of the optimization process. A test study considers the problem of an optimal blade design to maximize the aerodynamic performance of a low-speed fan. The approach employs a commercial CFD software, coupled with an unstructured mesh generator, as a response analysis tool. The ability of the applied Response Surface Optimization algorithm to find a global optimum of the objective function is examined.

Nomenclature

CP	-	Bezier control point
M	-	Meridional (axial) CP coordinate
M'	-	Normalized meridional CP coordinate ($M' = M/R$)
p	-	Thermodynamic (static) pressure
R	-	Fan radius
RSO	-	Response surface optimization algorithm
S	-	Fractional distance along a curve in the CFX-Bladegen coordinate system ($0 \leq S \leq 1$)
t	-	Time
t	-	Blade airfoil thickness
β	-	Tangential CP coordinate
δ	-	Displacement factor for CP meridional coordinate
ε	-	Efficiency
θ	-	Blade leading edge circumferential angular (LECA) coordinate
ξ	-	Airfoil stagger angle

¹ Research Associate, idahosau@erau.edu, Member AIAA

² Associate Professor, golub1b@erau.edu, Senior Member AIAA

³ Senior Development Engineer, vladimir@vrand.com, Senior Member AIAA

Subscripts:

abs	-	absolute frame of reference
h	-	hub location
LE	-	Leading edge
r	-	CP span layer index ($1 \leq r \leq 5$)
rel	-	relative frame of reference
s	-	CP meridional (axial) index ($1 \leq s \leq 4$)
S	-	Static
T	-	Total
TE	-	Trailing edge

I. Introduction

THE efforts to merge MDO and CFD technologies in application to engineering design of fluid system components have been rapidly increasing in recent years. This has been a particularly visible trend in the conceptual aircraft design, where, as stated in Ref. [1], with the availability of high performance computing platforms and robust numerical methods to simulate fluid flows, it became possible to shift attention from CFD development to automated design procedures combining CFD with optimization techniques in determining optimum aerodynamic designs. On the other hand, the major studies in this area were primarily devoted to the classical benchmark of an optimal aerodynamic design for a 2D airfoil, with the main efforts devoted to issues of the proper airfoil geometry parameterization and selection of an efficient optimization algorithm. In this regard, e.g., Fanjoy and Crossley [2] developed a method to optimize airfoil designs by using 21 design variables representing the control points of a B-spline, which appeared sufficient to reproduce nearly any arbitrary shape, but introduced geometric waves between control points translated to “wavy” velocity distribution in the analysis. A similar approach with 10 control point was employed by Pulliam et al. [3] in their comparison of genetic and adjoint methods for viscous airfoil optimization. Alternatives to the direct-design approach, including inverse methods to parameterize the geometry by matching it to the optimal flowfield conditions, were also developed [4]. For rotorcraft airfoils, a study on aeroacoustic optimization using a genetic algorithm was conducted in Ref. [5]. Using simplifying assumptions for low-order aeroacoustic analysis without structural constraints, a set of rotor airfoil shapes was generated representing a compromise between aerodynamic efficiency and minimum noise. Among the generated shapes, airfoils with *waves* on the upper and lower surfaces were predicted to produce reduction in the overall sound-pressure level. For 3D geometries, several recent works (e.g., Refs. [6-7]) addressed optimal wing and aircraft configurations, some using a multiobjective optimization strategy, and increasingly relying on evolutionary algorithms. Various methods to parameterize 3D geometries were analyzed, typically resulting in a large number of design variables to adequately represent the optimized shapes in terms of Bezier surfaces or B-splines. In one such study [8], a fuselage of a supersonic transport was parameterized in terms of 37 Bezier polygons, resulting, for an integrated wing-fuselage configuration, in 131 design variables. Various works also discussed automated grid generation procedures.

The design of highly efficient and quiet turbomachinery and generally propulsion system components represents a challenging task in many industrial applications ranging from aeropropulsion (e.g., turbofan and turboprop engines) to automotive and air-conditioning industries (e.g., cooling fans). The challenge is presented by the variety of flow and geometric parameters affecting the aerodynamic and acoustic performance, as well as the complexity of multi-scale unsteady flow-structure interaction phenomena, leading, e.g., to numerous noise-producing mechanisms and difficulty in their description and prediction.

In the present work, we address several critical issues related to the optimal design in turbomachinery by examining them in the context of the automated, industry-like MDO environment, developed and distributed on a parallel high-performance computer cluster. The main elements of any automated MDO system can be roughly subdivided into three major categories [9]: (i) CAD Modeling; (ii) Grid Generation; (iii) Design and Optimization Tools (including response sensitivity analysis). Each of these categories has been a focus of intensive research activities in recent years, aimed, in particular, at establishing transparent links for integrating all components in one automated, robust design and optimization process. The automated design systems thus must provide with the following capabilities [9]: (i) Use CAD for geometry creation; (ii) Generate grids automatically (black-box grid generation system); (iii) Use a common geometry representation for all disciplines involved in optimization process; (iv) Calculate analytical grid and geometry sensitivities; (v) Transfer data among disciplines consistently; (vi) Operate in an integrated system; (vii) Parameterize discipline models consistently. Below, we examine selected

aspects of these features as they are implemented in our integrated system and further in the test problem. We first review the main elements of our automated optimization system to illustrate its various capabilities, particularly related to the requirement to ensure a fully automated and efficient design optimization process. Next, we discuss the benchmark test study dealing with the optimal shape design of a fan blade. In this study, we employ CFD software coupled with an automated unstructured mesh generator, with objective to maximize the fan total efficiency. A procedure developed for the proper parameterization of the blade geometry to achieve the optimal blade design is discussed, and could be found particularly useful in a variety of industrial turbomachinery applications that employ the commercial CFD packages.

II. Automated MDO System

The essential elements of our industry-like, distributed, automated design optimization system include two software components developed by VR&D, Inc.: VisualDOC and DOT [10]. The primary component in most design optimization procedures, VisualDOC, is a graphics-based, general-purpose design optimization software system designed to interface easily to third-party analysis programs using its dedicated VisualScript interface. Design Optimization Tools (DOT) is a library of software modules that is designed to help solve a variety of nonlinear constrained or unconstrained optimization problems (used in many existing design optimization products, such as GENESIS, VisualDOC, MSC/NASTRAN, ADAMS, FEM5, POLYFEM, DAKOTA). VisualDOC's structure includes a graphical user interface (GUI), a database, and several functional modules. The central part of the system is the object-rational, multi-user, platform-independent database acting as a container for all design information. GUI allows launching design tasks, performing real-time monitoring of the optimization process, and post-processing results for various forms of design variables that may be in continuous, integer, discrete, or any combination forms.

A. Optimization Modules

The backbone of the optimization system is its functional modules performing the actual optimization, design study, etc. The menu includes the Gradient-Based Optimization (GBO), Design of Experiments (DOE), Response Surface Optimization (RSO), and Evolutionary Optimization (EO) modules.

GBO tools include extensively tested DOT software algorithms, such as sequential quadratic programming, modified method of feasible directions, sequential linear programming, Fletcher-Reeves, Broydon-Fletcher-Goldfarb-Shanno, and sequential unconstrained minimization technique methods, for various constrained and unconstrained multiobjective optimization problems. In the optimization process, VisualDOC calculates gradients of response-supplied cost functions and constraints using finite differences, but provides an option to employ user-supplied gradients.

Both DOE and RSO methodologies are used to establish empirical relationships between design variables and responses, which is a highly needed function in physical experiments and nonlinear analyses. They are also employed to filter out numerical noise from the analysis. According to Ref. [10], RSO has established itself as the most efficient method to use in optimization problems with relatively few (up to about 20) design variables, when the computational cost of performing a single analysis is high (a general trend in the growth of the number of terms in polynomial response surface models is shown in Figure 1). DOE works on the statistics of the design space distribution, thus helping to identify the design variables that have the most influence on the responses, and construct response surface approximations. A set of employed standard statistical DOE tools include full and fractional factorial, composite, simplex, Koshal, Box-Behnken, random, Latin Hypercube, Taguchi orthogonal arrays, D-optimal, and several other designs.

Finally, the Evolutionary Optimization module includes Genetic and Particle Swarm Optimization algorithms, which benefits include better chances of finding global optima while not requiring gradient information, and good handling of numerical noise.

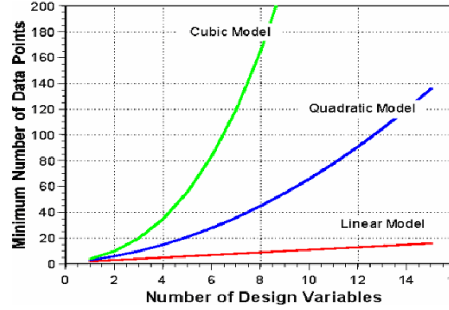


Figure 1: Influence of response surface models on number of design variables (courtesy VR&D, Inc.).

From the standpoint of the current test studies, one of the most important benefits of the system is its ability to efficiently interact with the third-party engineering analysis programs such as CFD and structural analysis tools. Such interaction is facilitated through a menu of interfaces, including ASCII-based Simple Text File Interface, multi-level Enhanced Text File Interface (VisualScript), and various specialized interfaces to MATLAB, Excel, and other analysis programs. Finally, another important VisualDOC’s feature, for application to complex optimization problems, is the system’s parallel computing capability. All the MDO functional modules, along with vectorized response analysis codes, have the ability to run in parallel on designated computer nodes using MPI message passing, thus creating a truly distributed environment. Although this feature has not been employed in the current benchmark tests, future studies will investigate effective use of the available networked cluster resources.

III. Test Study: Optimal Aerodynamic Design of a Fan Blade

The primary purpose of this project is to test the performance of the automated, distributed MDO/CFD environment designed for its future use in industrial turbomachinery MDO applications. We consider the task of an optimal blade design to maximize the total efficiency of an axial fan with uniform upstream flow using commercial CFD software, commonly employed in industrial turbomachinery design. The focus is on examining various approaches to the efficient parameterization of the blade geometry that would be most appropriate for the robust automated MDO process when employed in conjunction with a commercial CFD product. Contrary to the airfoil design studies, no guidelines have yet been established for the efficient parameterization of the three-dimensional blade geometry. The objective function for this study is the total efficiency (ε_T) of the fan blade, defined as:

$$\varepsilon_T \Big|_{LE-TE} = \left[\frac{\partial P_{T_{abs}}}{\partial P_{T_{abs}} + \partial P_{T_{rel}}} \right]_{avg}^{mass} \quad (1)$$

A. Commercial CFD Solver as a Response Analysis Tool

As a response analysis tool, we have selected BladeGenPlus software component from the CFX TurboPlatinum Package by ANSYS, Inc. (currently integrated in the ANSYS Workbench, Ref. [11]). This RANS CFD blade-passage solver is one of the most efficient commercial CFD analysis tools used in industrial turbomachinery design applications. BladeGenPlus is an integrated blade design software (BladeGen) coupled with the blade passage unstructured RANS solver. The software is integrated with VisualDOC in the automated optimization process governed by VisualScript.

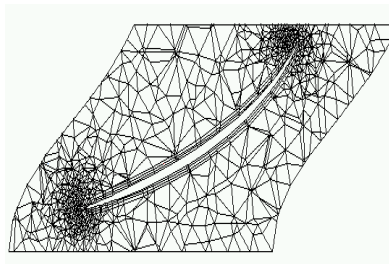


Figure 2: Sample unstructured mesh profile for CFD analysis

B. General Optimization Approach: Interaction of MDO Components

In the optimization process, the fan operating conditions are set either as specified parameters, or constraints in the optimization cycle, and include: (i) volumetric flow rate, (ii) range of safe (unstalled) fan operation, and (iii) fan static pressure rise. Fan diameter is usually prescribed as a geometric constraint. Additional geometric constraints are imposed on the design parameters used in the parameterization of the blade geometry. No structural constraints are imposed in this test study.

The initial task involves selection of proper parameters that completely and efficiently define the fan blade geometry (discussed in detail below). These parameters are then passed to the optimization module that generates another set of parameters describing a new, prospective blade design. At the next stages, the new blade geometry is generated in BladeGen, followed by an automated unstructured mesh generation, CFD analysis, and transfer of results to the optimization module. Figure 3 illustrates a general flowchart of the optimization process. In summary, the optimization task can be roughly subdivided into four major segments: (i) Generation of blade geometry using BladeGen software based on current input parameters; (ii) CFD analysis performed on a new blade design using BladeGenPlus; (iii) Passing results of CFD analysis to VisualDoc optimizer; (iv) Generation of a new set of design parameters based on an iterative step of the selected optimization algorithm. In what follows, we briefly describe some essential elements of the MDO process and their functions, with more details provided in Ref. [12].

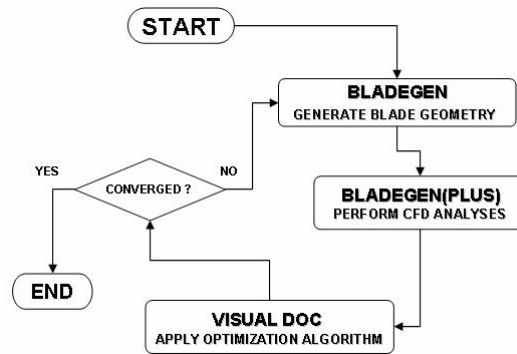


Figure 3: General MDO component flowchart

C. Parameterization of Blade Geometry

A critical step in the automated design optimization procedure is the selection of an efficient way to parametrically describe the blade geometry. The blade model is developed using the BladeGen turbomachinery component design utility from ANSYS, Inc. The coordinate system utilized in generating the three dimensional blade geometry is illustrated in Figure 4, where

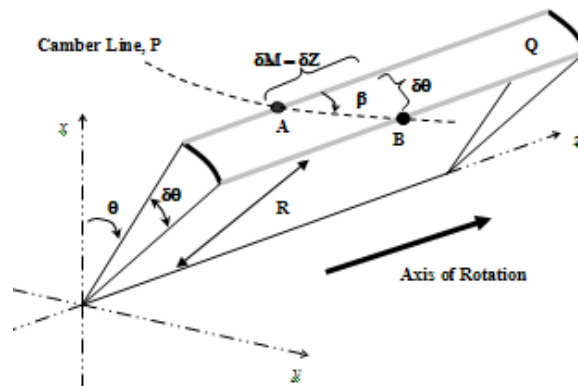


Figure 4: Blade geometry coordinate system

$$\delta M = \sqrt{\delta R \cdot \delta R + \delta Z \cdot \delta Z} \quad (2)$$

$$\beta = \tan^{-1}\left(\frac{\delta \theta}{\delta M'}\right) \quad (3)$$

- δM - differential meridional displacement;
- δR - differential radial displacement;
- δZ - differential axial displacement;
- $\delta \theta$ - blade leading edge circumferential angle (positive: x-towards-y);
- $\delta M'$ - meridional coordinate (δM) normalized by the radial coordinate, R (thus, $\delta M' = \delta M/R$).

In BladeGen, the blade model is defined by data points distributed over a number of user-specified constant-radius layers, spanning from 0% at the hub to 100% at the shroud. The geometrical properties, including blade angles and thickness distributions, are then specified at each spanwise layer, and interpolations between layers are employed to generate the three-dimensional geometry.

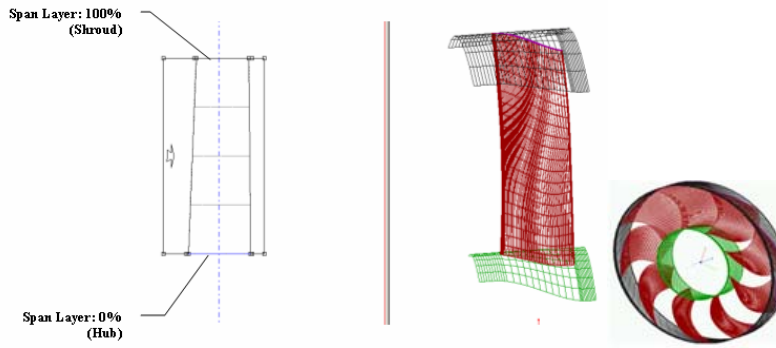


Figure 5: Meridional View (LHS) of Fan with Span Layers Visible

At each span layer, the blade section (airfoil) is created using the BladeGen coordinate system to specify a set of points which represent the camberline (meanline) of the blade section at that span layer. The camberline coordinates are specified using a “ β - M ” distribution from the leading edge (LE) to the trailing edge (TE). A thickness distribution is then superimposed on the camberline to create the complete profile of the blade section. A standard NACA 0012 thickness distribution is used for all the models in this test study in order to reduce the number of design parameters. A separate study investigating the effect of thickness distribution is anticipated in the future.

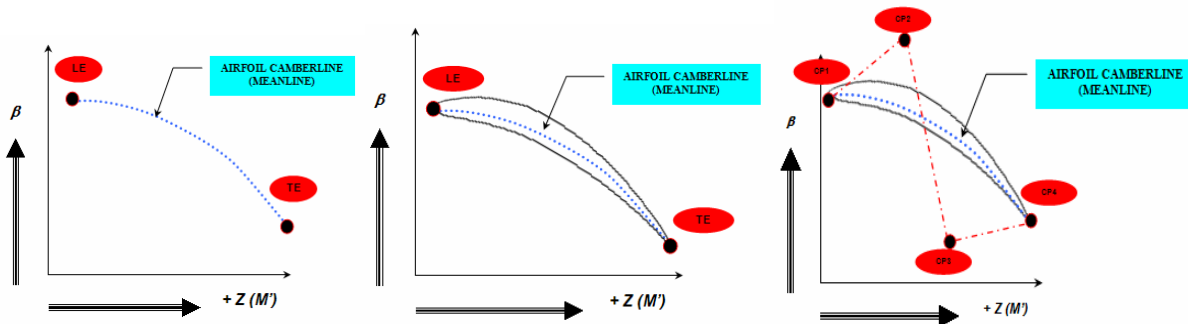


Figure 6: Blade profile generation at constant radius span layer

The methodology for generating the blade profile is illustrated in Figure 6 and further below. In Figure 6(a), the camberline is shown in the “ β - M ” coordinate system. Figure 6(b) shows the camberline along with the superimposed blade thickness distribution. In Figure 6(c), a 3rd order Bezier control polygon is generated to control the shape of the blade section camberline. The use of the Bezier control polygon is to ensure that the camberline is smooth and free of discontinuities, a necessary requirement for generating valid blade geometries.

The coordinates of the control points (CPs) that describe the Bezier control polygon are used as design parameters in the design optimization study. A total of 5 span layers are specified to generate the blade geometry. A distinct Bezier polygon is necessary to generate the blade profile using each of the five span layers. Four x-y coordinate pairs corresponding to the β -M BladeGen coordinates are required for each of the 5 Bezier polygons, yielding a total of 40 design parameters (5 Span layers * 4 coordinate *pairs*). In essence, the blade geometry “control grid” is generated which consists of β -M coordinates of all the Bezier control polygons for each of the 5 span layers, as illustrated in Figure 7.

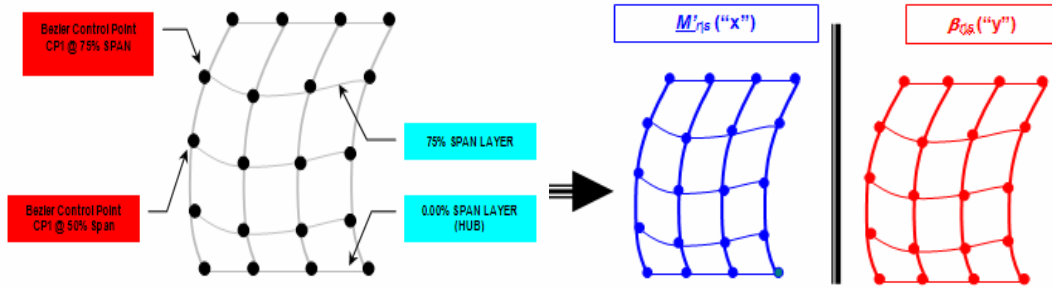


Figure 7: Blade geometry “control grid” with Bezier coordinates for camberlines at all span layers

In order to appropriately locate Bezier control points on the grid, an indexing system is developed that employs the “ r/s ” subscripts to indicate the location of the control points. The subscript r designates the span layer at which the CP resides ($1 \leq r \leq 5$). The subscript s designates the index of the CP along the Bezier polygon ($1 \leq s \leq 4$) (i.e., the LE line control points have an index of 1, while the TE line of the Bezier polygon has an index of 4). The use of the Bezier polygons to generate the blade profiles at each span layer provides the ability to specify the hub-to-shroud twist variation of the blade model. The hub-to-shroud sweep of the LE line of the blade is specified using the LE circumferential angle (θ). This angle (LECA) is specified at each span layer from the hub to the shroud, which defines the circumferential sweep distribution of the blade, as illustrated in Figure 8. The 5 LECAs, combined with the 40 Bezier coordinate control points, result in a total of 45 design parameters specifying the blade geometry.

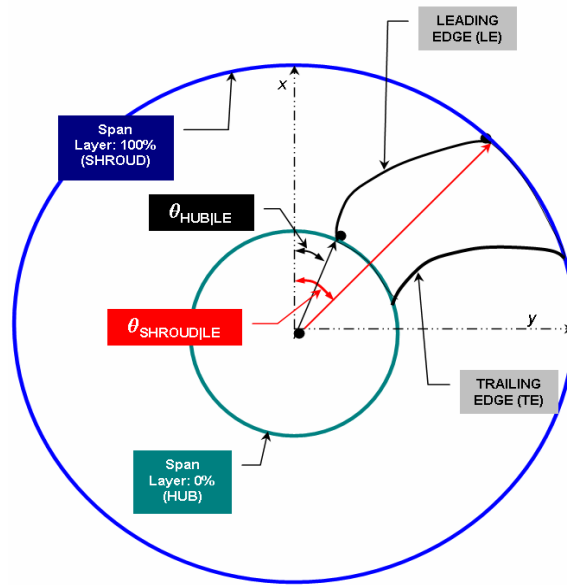


Figure 8: Nomenclature for blade circumferential sweep

D. Constraints on Design Variables

The number of design variables (45) in the initial blade parameterization scheme can be decreased by applying certain constraints. The first set of constraints involves fixing the $M'(x)$ coordinates of the Bezier control points specified along the blade leading and trailing edge lines (10 coordinates). The $\beta(y)$ coordinates of the LE line Bezier control points are also held constant (5 coordinates). The primary reasons for fixing the LE Bezier coordinates is to ensure that the blade angles along the leading edge line match those specified based on the blade vortex models used to generate the initial blade designs. These constraints eliminated a total of 15 design parameters, thus leaving 30 design variables.

An additional modification to the parameterization scheme is made to ensure that the third Bezier control point always follows the second Bezier control point when the polygon is generated. This is achieved by generating the meridional coordinates of the third Bezier CP using a *displacement factor*, δ , and applying the following relationship at each span layer:

$$M'_{r|3} = M'_{r|2} + (90 - M'_{r|2})\delta_r + 5 \quad (4)$$

with limits $10 \leq M'_{r|2} \leq 80$ and $0 \leq \delta_r \leq 1$, where δ_r is the displacement factor at a span layer with index r .

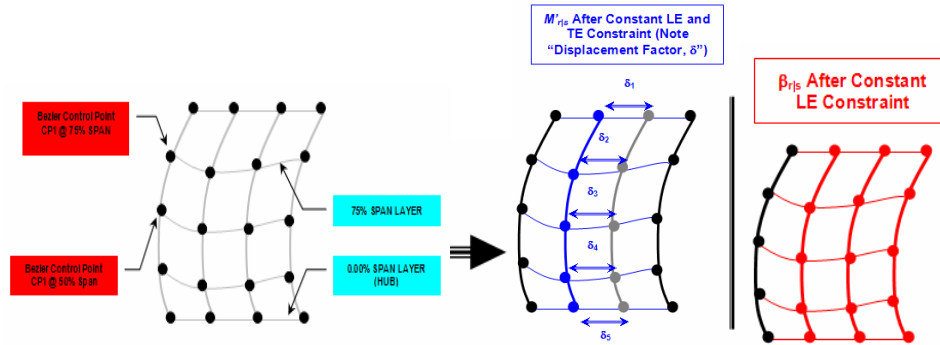


Figure 9: Blade geometry control grid (constrained coordinates are shown in black on the right)

The modified control grid for the blade geometry with constrained (black) and unconstrained (colored) $M'(x)$ and $\beta(y)$ Bezier coordinate points is shown in Figure 9. The resulting effect is the reduction of the actual Bezier design variables from 40 to 25 (compare with Figure 7), with additional constraints imposed on the relative positions of the coordinate points residing at the adjacent span layers. Combined with 5 LECA variables, the total number of the design variable specifying the blade geometry is 30.

In the optimization study, the number of fan blades, and the rotational speed (RPM) of the fan, are included as design variables, for a total of 32 design parameters.

E. Automated Response Analysis Procedure

It is essential to maintain the response analysis stage as a completely automated, non-interactive segment of the optimization process. To this end, a set of batch executable utilities is implemented to accomplish the goal. In particular, the following BladeGenPlus utilities are employed:

- *BladeBatch* converts the optimizer-generated, ASCII-based blade model into the BladeGen design format;
- *BgBatch* applies new operating parameters, such as the fan RPM and upstream flow conditions, to the model;
- *BgGrid* generates unstructured blade-passage mesh for the new BladeGen model;
- *BgSolve* performs a CFD analysis of the blade passage and stores results in a specified file;
- *BgExtract* extracts computational results from the *BgSolve* output file and stores them in a specified file.

The need for completely automated optimization and response analysis procedures implies a considerable level of robustness to be built in the MDO environment, allowing it to handle extreme design cases. To this end, MATLAB scripts are developed to handle the following issues identified as critical to the robustness of the MDO methodology:

- Invalidity of extremely twisted, swept or distorted blade designs is communicated to the optimization module through the Geometry Pass/Fail parameter;
- Information on blade designs for which mesh could not be successfully generated is passed to the optimization module through the Grid Pass/Fail parameter;
- Invalidity of CFD results stored in the response analysis file is communicated to the optimization module through the CFD Pass/Fail parameter.

Note that the availability of the Pass/Fail parameter in VisualDOC, complemented with the software's ability to easily interface with MATLAB scripts, allows for a considerable robustness of the automated MDO process, as the latter is not immediately terminated in the event of problems associated with invalid blade designs, unsuccessful mesh generation, or unsuccessful CFD analysis (in all cases, the optimization process automatically recovers and continues).

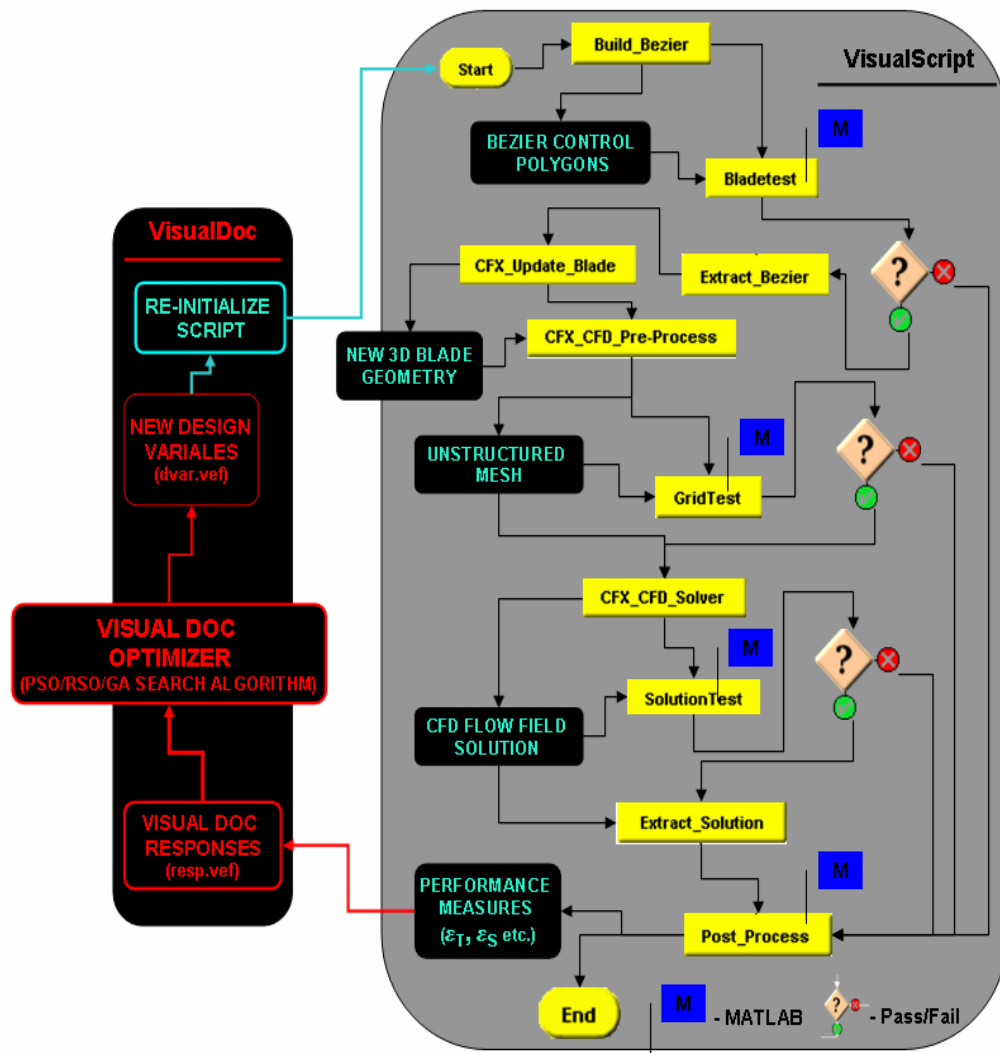


Figure 10: Details of the automated MDO process

Index	Name	Type	Objective	Constraint	Low Bound	Upp Bound
1	PFBldetest	Pass/Fail	<input type="checkbox"/>	<input checked="" type="checkbox"/>	0.00	None
2	PFGrid	Pass/Fail	<input type="checkbox"/>	<input checked="" type="checkbox"/>	0.00	None
3	PFRResults	Pass/Fail	<input type="checkbox"/>	<input checked="" type="checkbox"/>	0.00	None
4	MassFlowRate	Independent	<input type="checkbox"/>	<input type="checkbox"/>	None	None
5	VolFlowRate	Independent	<input type="checkbox"/>	<input checked="" type="checkbox"/>	3.00	6.00
6	TotBlTorq	Independent	<input type="checkbox"/>	<input type="checkbox"/>	None	None
7	Headrise	Independent	<input type="checkbox"/>	<input type="checkbox"/>	None	None
8	InFlowCoeff	Independent	<input type="checkbox"/>	<input type="checkbox"/>	None	None
9	ExFlowCoeff	Independent	<input type="checkbox"/>	<input type="checkbox"/>	None	None
10	HeadCoeff	Independent	<input type="checkbox"/>	<input type="checkbox"/>	None	None
11	TotalEffic	Independent	<input checked="" type="checkbox"/>	<input checked="" type="checkbox"/>	0.25	1.00
12	StaticEffic	Independent	<input type="checkbox"/>	<input checked="" type="checkbox"/>	0.00	1.00

Figure 11: VisualDoc’s specification of the case parameters

The optimization module of the design process detailed in Figure 10 consists of the VisualDoc and VisualScript components. VisualDoc controls implementation of the selected optimization algorithm whose results are based on the CFD response analysis of the previous design iteration. A new set of design variables is generated by VisualDoc, and transferred for further analysis as part of the MDO process governed by VisualScript. The latter is thus responsible for all calls to various batch utilities performing critical analysis tasks, including the blade geometry modeling, grid generation, CFD analysis, and transfer of the CFD results to the optimizer.

Figure 11 shows the design variables and response parameters in the test study, as specified in the VisualDoc’s graphical user interface (GUI). The responses include the target function (total efficiency) along with other performance characteristics such as the fan head rise, blade torque and static efficiency (more details are provided in Ref. [12]).

F. Selection of Optimization Algorithm

The response surface optimization (RSO) algorithm has been selected for the test study. RSO has established itself as a more efficient method when the computational cost of performing a single analysis is rather high [10], which is the case in the current MDO study. On the other hand, the RSO algorithm is more effective when the number of design variables is *not* too high (Figure 1 illustrates a nonlinear growth in the required number of data points, i.e., calls for the response analysis, as the number of variables increases). This effect is even more pronounced for more accurate, higher-order response surface models.

In order to increase the efficiency of the RSO algorithm in the current study, the 32 design variables are grouped into subsets. The blade design is thus sequentially optimized relative to the subsets of the design variables (i.e., the blade design is first optimized relative to the first subset, with the best obtained design then optimized relative to the second subset, etc.). The process is carried out iteratively until no appreciable increase in the objective function can be obtained. Table 1 shows the employed subsets of design variables, and the order in which the optimization on the subsets is performed.

ORDER	VARIABLES (Unless otherwise specified, $r = 1..5$)	TOTAL #
1	β coordinates of interior Bezier control points ($\beta_{r,2}, \beta_{r,3}$)	10
2	Circumferential LE sweep angle (θ_r)	5
3	Meridional coordinate of CP2 ($M'_{r,2}$)	5
4	Displacement factor for CP3 meridional coordinate (δ_r)	5
5	β coordinates of TE Bezier control points ($\beta_{r,4}$)	5
6	Fan RPM and number of blades.	2

Table 1: Subsets of design variables in the MDO study

VisualDoc's implementation of the RSO algorithm requires that bounds are imposed on the design variables and response parameters, in order to define the design space within which the response surface is generated. The bounds imposed in the current study are shown in Table 2. Additional restrictions and included in Table 3 with the purpose of selecting a more accurate (quadratic) response model without imposing excessively stringent optimization convergence criteria.

DESIGN VARIABLE	LOWER BOUND	UPPER BOUNDS	RESPONSE PARAMETER	LOWER BOUND	UPPER BOUND
# of Blades	2	20	PFBladetest	0	None
RPM	-1500	-500	PFGrid	0	None
δ_r	0	1	PFResults	0	None
$M'_{r/2}$	10	80	VolFlowRate(m ³ /s)	3.00	6.00
$\beta_{r/s}$	SP* - 40 (10) ⁺	SP* +40 (80) ⁺	Total Efficiency	0.25	1.00
θ_r	-30	30	Static Efficiency	0.00	1.00

* SP – Starting point of Bezier coordinate (from base design)
+ Min/Max value (used if computed bound exceeds this value)
Unless otherwise stated, $1 \leq r \leq 5$ and $1 \leq s \leq 4$

Table 2: Upper and lower bounds for design variables and response parameters in MDO study

Min Number of Design Points	4
Max Number of Design Points	106
Number of User Supplied Design Points	1
Order of Approximations	Full Quadratic
Generate Initial Points	Simplex Design
Consecutive Iterations for Convergence	5
Initial Quadratic Relative Move Limit	0.2
Quadratic Absolute Move Limit	0.02
Relative Objective Convergence Tolerance	0.001
Absolute Objective Convergence Tolerance	0.0001
Relative Design Variable Convergence Tolerance	0.001
Absolute Design Variable Convergence Tolerance	0.0001
Constraint Tolerance	-0.03
Violated Constraint Tolerance	0.003
Objective	Maximize

Table 3: Parameters of the Response Surface model and optimization convergence criteria

III. Results of the MDO Test Study

In the MDO study, three base fan models (prototypes) are used to examine the ability of the MDO algorithm to converge to a globally optimal fan design. We first discuss optimization results obtained for each base design, and further compare them. The three base designs used in the MDO study are shown in Table 4.

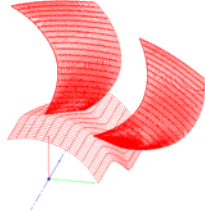
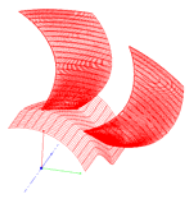
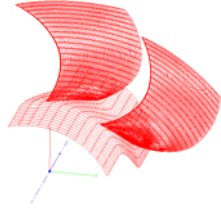
	MODEL1	MODEL2	MODEL3
			
Rotational Speed (RPM)	1140	1720	1140
Diameter (in)	30	24.3	30
Number of Blades	9	9	9
R_{hub}/R_{tip}	0.4	0.4	0.45
Chord Ratio C_{tip}/C_{hub}	2	2	1.88

Table 4: Fan prototype models

A. MDO Results for Model 1

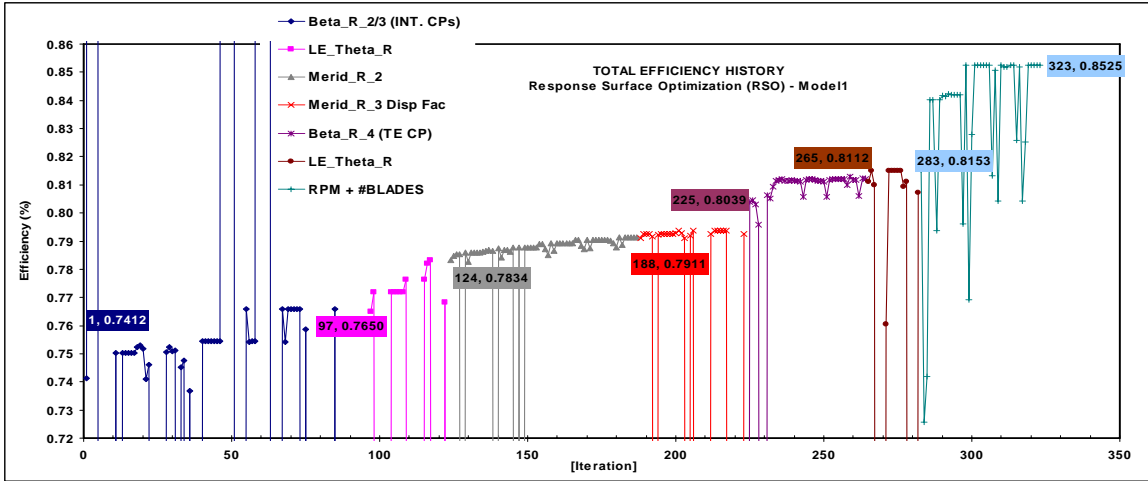


Figure 12: Target function plot for Model 1

Figure 12 illustrates the history plot of the target function (efficiency) for Model 1 based on the sequential design optimization conducted on the subsets of design variable. Figure 13 summarizes the efficiency gains obtained for each subset, and compares the base and the optimized fan geometries. Note a remarkable wavy shape of the leading edge line in the optimized blade design. The total efficiency gain for Model 1 is approximately 11% after 323 design iterations. The largest gain in efficiency is obtained from the simultaneous variation of the fan rotational speed (RPM) and the number of blades. In terms of the Bezier geometry variables, the largest efficiency gain is obtained from variations of the blade β coordinates. In order to re-examine the method of sequential subset optimization employed in the study, an additional round of design iterations is conducted by separately varying the sweep distribution of the blade LE line. The efficiency gain of 0.41% (compared to the original 1.84%) suggests that the method may indeed be successful, provided that the proper subsets of design variables are identified.

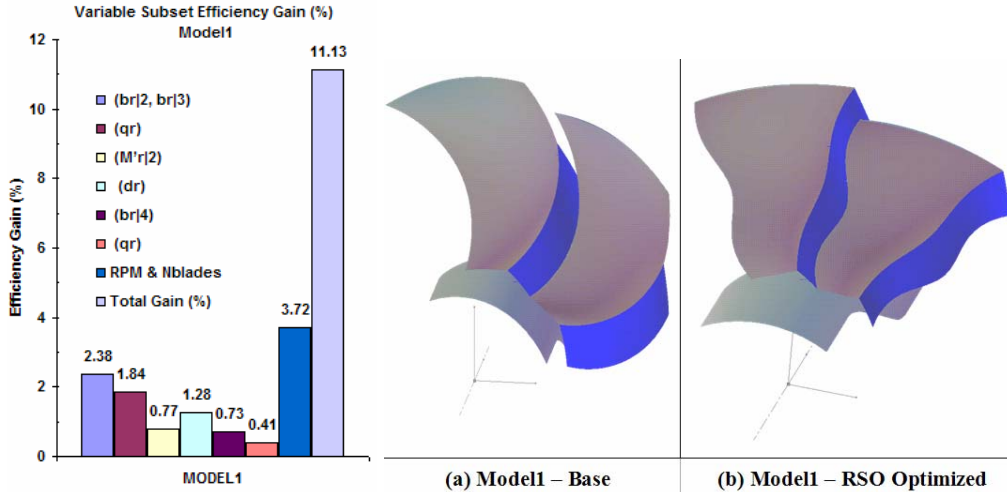


Figure 13: RSO optimization results for Model 1

B. MDO Results for Model 2

Similar to the previous case, the design optimization of Model 2 (Figures 14 and 15) results in the wavy blade LE line. The efficiency gain plots also show that the simultaneous variation of the RPM and the number of blades yields the largest efficiency gain of 9%. The variation of the leading edge sweep (qr) and the β coordinates of the Bezier control points (br*i*) produces higher efficiency, compared to the gains obtained from the meridional ($M^r_{r|s}$ and dr) Bezier CP coordinates.

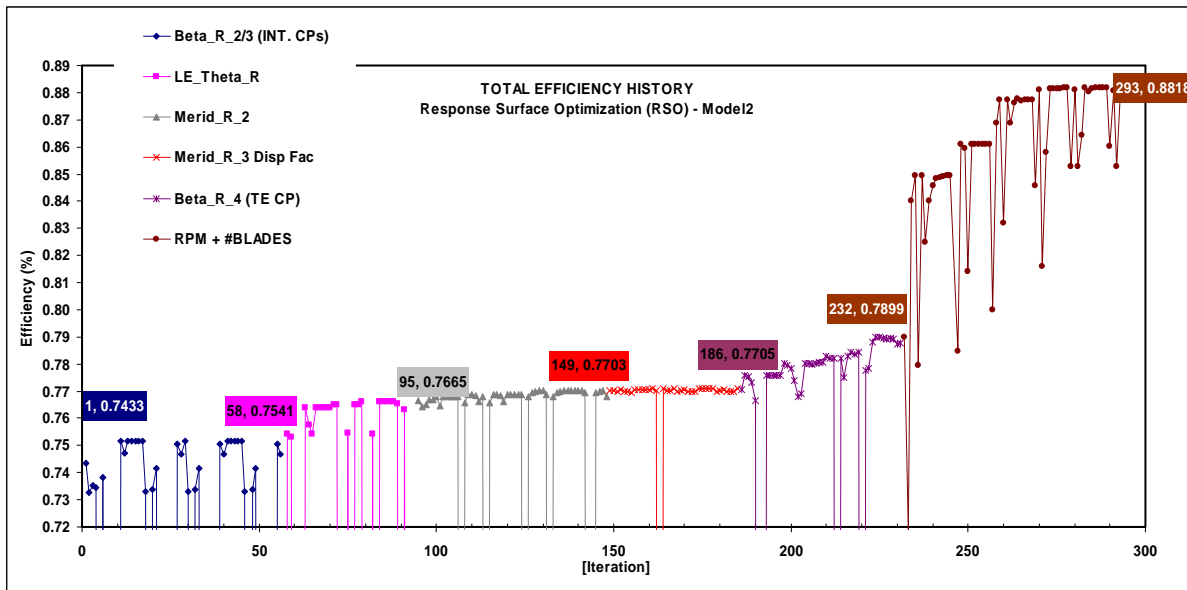


Figure 14: Target function plot for Model 2

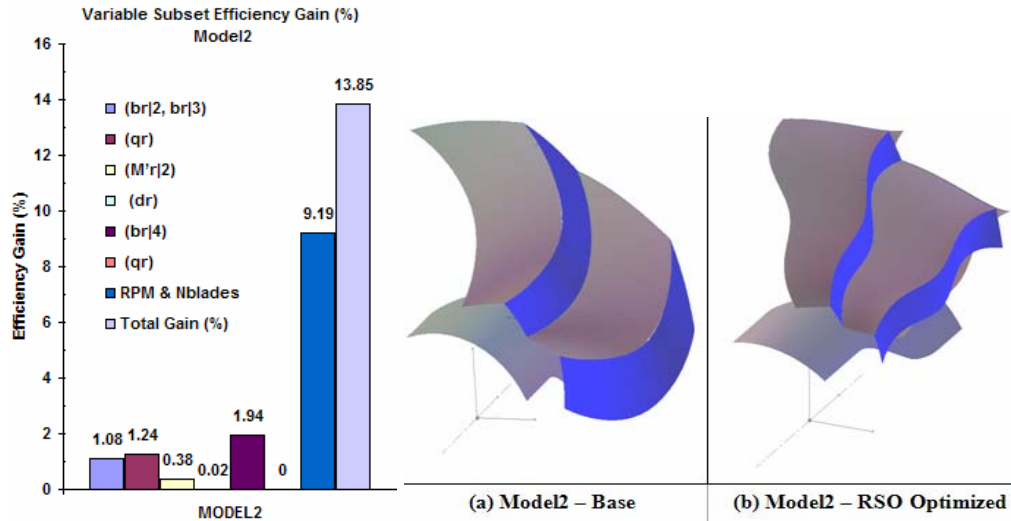


Figure 15: RSO optimization results for Model 2

C. MDO Results for Model 3

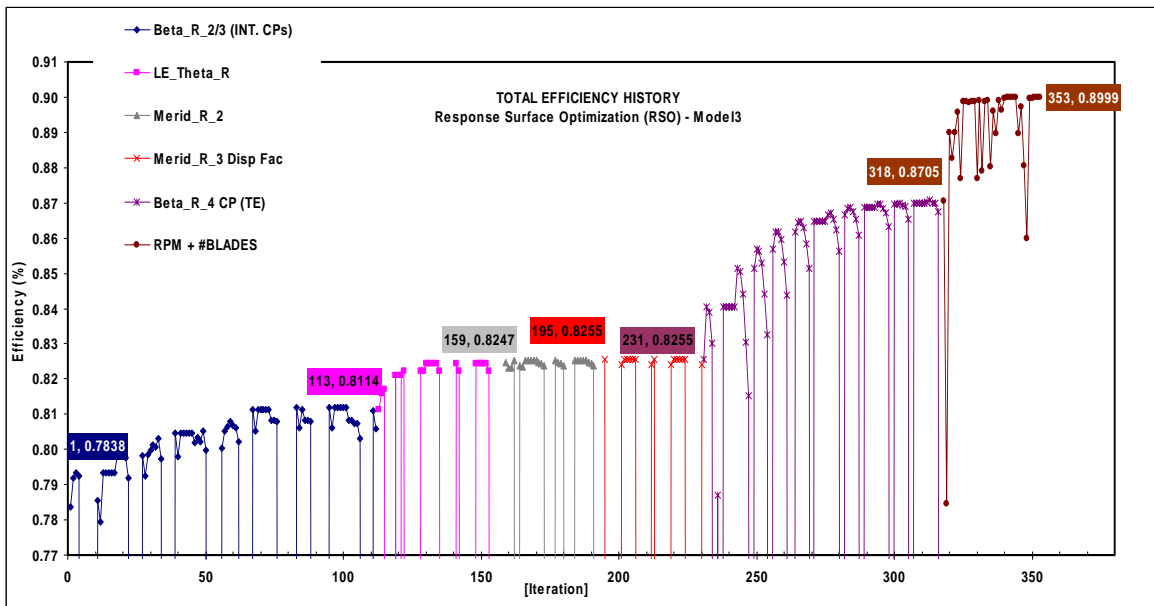


Figure 16: Target function plot for Model 3

The results observed in Figures 16 and 17 for Model 3 also show similarity to those obtained for the previous two models. The wavy leading edge shape is evident, with the efficiency gain plots showing an increase of 11.6%. The largest efficiency gain for this model (4.5%) is obtained from the variation of the β coordinates for the TE Bezier control point. Large efficiency gains are also obtained from the simultaneous variation of the fan RPM and the number of blades, as for the previous two models. Finally, in agreement with the previous results, the fan efficiency appears to be much more sensitive to variations of the β coordinates of Bezier control points, compared to the effect from the corresponding meridional coordinates.

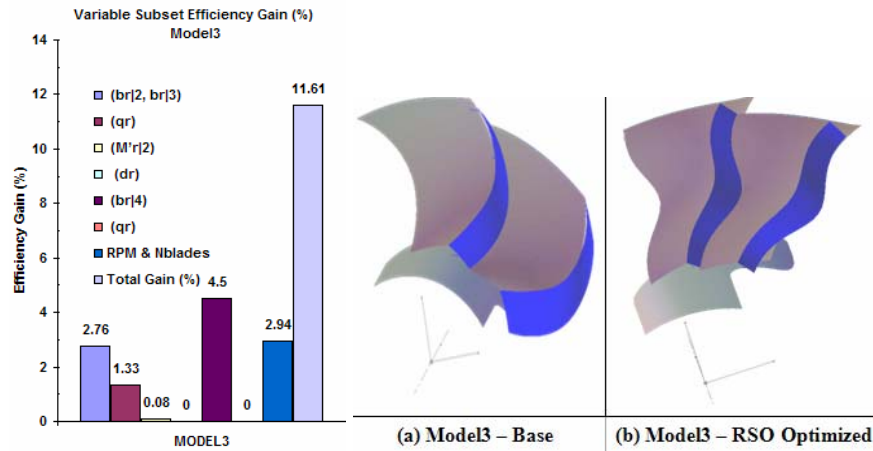


Figure 17: RSO optimization results for Model 3

D. Comparison of Results

Figure 18 and Table 5 compare the efficiency gains for the three base models. In general, the results identify the β coordinates of the Bezier control points, and the fan rotational speed and the number of blades, as the critical design variables with the most significant influence on the target function (total fan efficiency). An average efficiency gain of 12 % is obtained for the three base models. The appearance of the wavy shape of the leading edge line in the optimized models needs to be further investigated to determine if this effect is rather related to the specific choice of the blade parameterization scheme.

To conclude on the ability of the RSO algorithm to identify a globally optimal blade design, a comparison of the optimized models is presented in Table 5 that shows a noticeable variation between the three resulting designs. Further studies will examine if those are primarily related, e.g., to the initial differences in the fan diameters and/or the hub-tip ratios of the original models. On the other hand, the resulting large numbers of blades in the final designs could be due to the absence of constraints on the total blade torque, forcing the optimizer to increase the solidity of the fan designs.

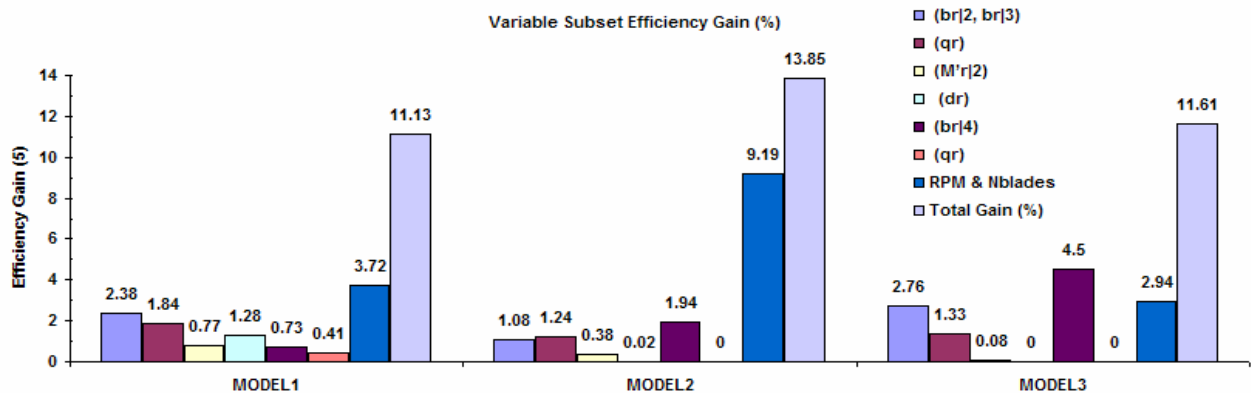


Figure 18: Summary of efficiency gains for three models

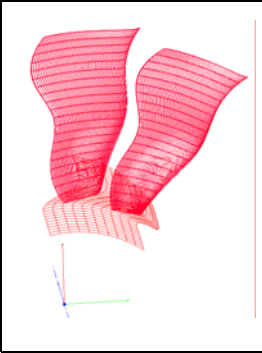
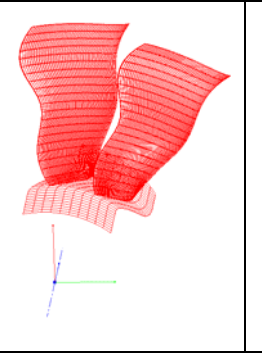
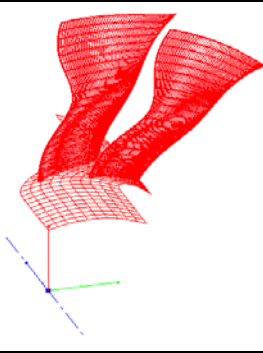
			
	Model1	Model2	Model3
RPM	972	1287	1193
# Blades	12	15	17
VFR (m³/s)	3.616	3.30	4.96
Torque (Nm)	17.85	13.41	38.61
Head Rise (m)	37.66	42.59	76.78
Static Effic. (\mathcal{E}_{ST})	0.598	0.660	0.608
Total Effic. (\mathcal{E}_T)	0.871	0.902	0.917
Total Effic. Gain ($\delta\mathcal{E}_T$)	+ 10%	+7.8%	+10%
δP_{Tabs} (MPa)	$0.438e^{-3}$	$0.495e^{-3}$	$0.892e^{-3}$
dP_{Trel}	$-0.064e^{-3}$	$-0.054e^{-3}$	$-0.080e^{-3}$
dP_{st}	$0.301e^{-3}$	$0.362e^{-3}$	$0.592e^{-3}$

Table 5: Comparison of optimized fan designs

V. Summary

In this work, we examined an approach to the optimal blade design using the developed automated, industry-like multidisciplinary design optimization (MDO) environment. In a benchmark test study, we employed a commercial CFD software (coupled with an automated unstructured mesh generator) as a response analysis tool in a constrained, automated design optimization process, with the objective to maximize the fan total efficiency. The study examined the ability of the response surface optimization (RSO) algorithm to find a globally optimal design. The project served as a benchmark for testing the performance of the developed MDO environment, and addressed numerous issues in the automated optimization procedure, such as those related to the proper blade geometry parameterization, algorithm selection, and transparent interconnections between different elements of the design optimization process.

VI. References

1. Jameson, A., "Essential Elements of Computational Algorithms for Aerodynamic Analysis and Design," NASA/CR-97-206268, 1997.
2. Fanjoy, D.W. and Crossley, W.A., "Aerodynamic Shape Design for Rotor Airfoils via Genetic Algorithm," J. of American Helicopter Society, Vol.43, pp.263-270, 1998.
3. Pulliam, T.H., Nemec, M., Holst, T. and Zingg, D.W., "Comparison of Evolutionary (Genetic) Algorithm and Adjoint Methods for Multi-Objective Viscous Airfoil Optimizations," AIAA Paper 2003-298.
4. Gardner, B.A. and Selig, S.S., "Airfoil Design Using a Genetic Algorithm and an Inverse Method," AIAA Paper 2003-0043.

5. Jones, B.R., Crossley, W.A. and Lyrintzis, A.S., "Aerodynamic and Aeroacoustic Optimization of Rotorcraft Airfoils via a Parallel Genetic Algorithm," *Journal of Aircraft*, Vol.37, 2000.
6. Cliff, S.E., Reuter, J.J., Saunders, D.A. and Hicks, R.M., "Single-Point and Multipoint Aerodynamic Shape Optimization of High-Speed Civil Transport," *Journal of Aircraft*, Vol.38, 2001.
7. Sasaki, D., Obayashi, S. and Nakahashi, K., "Navier-Stokes Optimization of Supersonic Wings with Four Objectives Using Evolutionary Algorithm," *Journal of Aircraft*, Vol. 39, 2001.
8. Sasaki, D., Yang, G. and Obayashi, S., "Automated Aerodynamic Optimization System for SST Wing-Body Configuration," AIAA Paper 2002-5549.
9. Samareh, J.A., "Geometry Modeling and Grid Generation for Design and Optimization," Keynote Lecture at ICASE/LaRC/NSF/ARO Workshop on Computational Aerosciences in the 21st Century, April 22-24, 1998.
10. Balabanov, V.O., Charpentier, C., Ghosh, D., Quinn, G., Vanderplaats, G., and Venter, G., "VisualDOC: A Software System for General-Purpose Integration and Design Optimization," AIAA Paper 2002-5513.
11. <http://www.ansys.com/products/>
12. Idahosa, U.O., "An Automated Optimal Design of a Fan Blade Using an Integrated CFD/MDO Computer Environment", *M.S.A.E. Thesis*, Embry Riddle Aeronautical University, Daytona Beach, Florida, 2005